IOP Conf. Series: Materials Science and Engineering **47** (2013) 012054 doi:10.1088/1757-899X/47/1/012054

Structure and performance of polymer-derived bulk ceramics determined by method of filler incorporation

T Konegger[1], P Schneider[1], V Bauer[1], A Amsüss[1] and A Liersch[2]

[1] Institute of Chemical Technologies and Analytics, Vienna University of Technology, 1060 Vienna, Austria
[2] Department Materials Science, Glass and Ceramics, Koblenz University of Applied Sciences, 56203 Höhr-Grenzhausen, Germany

E-mail: thomas.konegger@tuwien.ac.at

Abstract. The effect of four distinct methods of incorporating fillers into a preceramic polymer matrix was investigated with respect to the structural and mechanical properties of the resulting materials. Investigations were conducted with a polysiloxane/Al_2O_3/ZrO_2 model system used as a precursor for mullite/ZrO_2 composites. A quantitative evaluation of the uniformity of filler distribution was obtained by employing a novel image analysis. While solvent-free mixing led to a heterogeneous distribution of constituents resulting in limited mechanical property values, a strong improvement of material homogeneity and properties was obtained by using solvent-assisted methods. The results demonstrate the importance of the processing route on final characteristics of polymer-derived ceramics.

1. Introduction

Polymer-derived ceramics (PDCs) present a viable alternative to conventional ceramics due to the multitude of processing options available. This results in the ability to produce structures as diverse as coatings, cellular materials, fibers, or bulk materials [1]. In order to overcome the intrinsic problem of high shrinkage during polymer-to-ceramic transformation, fillers are generally applied, thus reducing shrinkage and, subsequently, the tendency of crack formation during pyrolytic conversion of bulk materials [2]. Furthermore, fillers can be applied as reagents in PDCs, reacting with the preceramic polymer or products thereof, and yielding novel compounds. Mullite ($3Al_2O_3 \cdot 2SiO_2$), for example, has been obtained from a reaction of polymer-derived SiO_2 with particulate Al_2O_3 [3]. Mullite is an important structural and high-temperature material owing primarily to its excellent thermal properties. A possibility to improve the limited mechanical performance of mullite-based systems, specifically in terms of strength and toughness, is the incorporation of ZrO_2 into the mullite matrix [4]. The formation of mullite/ZrO_2 composites using preceramic polymers with nanoscaled fillers has been reported recently [5].

The incorporation of particulate fillers into the matrix composed of the polymer precursor represents an important step during processing, strongly affecting the resulting composition and properties of the material. The objective of this work is the investigation of four distinct methods of introducing Al_2O_3 and ZrO_2 particulate fillers into a preceramic polysiloxane matrix, and to investigate the effect of the respective method on structural and mechanical properties of the obtained mullite/ZrO_2 composites. Furthermore, a novel approach for an effective quantitative determination of the uniformity of the filler distribution based on an image analysis approach shall be presented.

2. Experimental

2.1. Sample preparation

A commercially available poly(methyl)silsesquioxane (Silres® MK, Wacker Chemie AG, Germany) was used as preceramic polymer component. The solid thermosetting polymer powder with a nominal formula of $(CH_3SiO_{1.5})_n$ can be transformed into SiO_2 with a yield of 82 m.% after complete oxidation [6]. To promote cross-linking, a cross-linking agent (aluminum acetylacetonate, Merck; 1 m.% with respect to the polymer) was added. Al_2O_3 (CT 3000 SG, Almatis GmbH, Germany; d50 = 0.5 µm) and ZrO_2 (3Y, Treibacher Industrie AG, Austria; d50 = 0.4 µm) were used as fillers. For all samples, the same composition was used (23.4 m.% preceramic polymer, 47.9 m.% Al_2O_3, 28.7 m.% ZrO_2), resulting in a nominal composition of 50 m.% Al_2O_3, 30 m.% ZrO_2, and 20 m.% SiO_2 after full oxidation. Before addition to the polymer, corresponding amounts of the fillers were mixed in acetone, attrition milled for a duration of 2 h (PE 075, Netzsch, Germany; ZrO_2 milling media, stirrer, and lining), dried, sieved, and stored at 200 °C. Four distinct methods of filler incorporation were investigated.

Dry-mixing (DrM): Polymer, cross-linking agent and fillers were mixed in a tumble mixer (Turbula, Willy A. Bachofen AG, Switzerland) for 1 h at room temperature. Subsequently, the mixed powders were sieved (200 µm mesh size).

Melt-mixing (MeM): The polymer was heated to 120 °C yielding a viscous polymer melt, stirred with a dissolver stirrer, and the preheated fillers were slowly added forming a solid composite aggregate. The mixture, together with the cross-linking agent, was ball-milled for 1 h using ZrO_2 milling media, and sieved (200 µm mesh size).

Solvent-assisted coating (SoC): The filler powders were added to a solution of polymer and cross-linking agent in acetone. The mixture was stirred and ultra-sonicated before the solvent was removed in a rotary evaporator at 40 °C in vacuum. The resulting dried mixture was ball-milled for 1 h before sieving (200 µm mesh size).

Spray-coating (SpC): The polymer and the cross-linking agent were dissolved in acetone before the filler powders were added, preparing a slurry with a solid loading of 33 m.%. The slurry was stirred, ultra-sonicated, and spray dried in a laboratory scale spray drier (B-290, Büchi, Switzerland) in N_2 atmosphere at a gas flow temperature of 55 °C, yielding toroidal- to spherical-shaped granules with diameters up to 50 µm.

The resulting polymer/filler mixtures were uniaxially warm-pressed (200 °C, 50 MPa, 1 h) yielding cylindrical specimens with a diameter of 40 mm and a height of 4 mm. After warm-pressing and green machining, the pyrolytic conversion was conducted in a continuous Ar flow of 0.5 L min^{-1} at 800 °C for a duration of 4 h (1 K min^{-1} to 300 °C with a holding segment of 30 min; 0.6 K min^{-1} to 800 °C; cooling rate 3 K min^{-1}). For final consolidation, the pyrolyzed specimens were treated in air at 1600 °C for a duration of 1 h with an additional oxidation plateau at 1000 °C for a duration of 4 h (3 K min^{-1} to 300 °C, 0.6 K min^{-1} to 1000 °C, 1 K min^{-1} to 1600 °C, cooling rate: 3 K min^{-1}).

2.2. Structural and mechanical properties

The green density of the warm-pressed specimens was derived from the geometric dimensions and sample mass. In order to obtain the relative green density, the theoretical green density was calculated according to the rule of mixtures, taking into account the densities of the constituents ($\rho_{polymer}$ = 1.33 g cm^{-3}, ρ_{Al2O3} = 3.98 g cm^{-3}, ρ_{ZrO2} = 6.05 g cm^{-3}). The green strength was determined using a three-point flexural test with sample dimensions of 3 x 4 x 30 mm^3, a spanning width of 20 mm and a cross-head speed of 0.5 mm min^{-1}, averaging three test specimens per sample.

After sintering, the bulk density was determined employing Archimedes' principle. Furthermore, the apparent density was obtained by helium pycnometry (Ultrapycnometer 1000, Quantachrome, Germany). The crystalline phase composition of the sample bulk was determined by X-ray diffraction (XRD) analysis with Cu Kα radiation (X'Pert PRO, PANalytical, Netherlands). Quantification of the crystalline phase composition was determined by Rietveld refinement of the XRD data obtained,

employing the TOPAS software package (Topas R 2.1, Bruker). Ceramographic analyses were carried out by scanning electron microscopy (SEM, Quanta 200, FEI, Netherlands) of epoxy-embedded sample cross-sections polished to a finish of 1 µm with diamond media. Hardness was determined on the same polished samples by the Vickers method applying a load of 98.1 N (HV_{10}; M4V, Emco-Test, Austria), averaging a minimum of five individual tests per sample. The fracture toughness was calculated from the length of cracks which developed during the Vickers indentation test according to the relation proposed by Niihara assuming Palmqvist cracks [7]. Young's moduli were determined employing the impulse excitation technique using rectangular sample geometries (RFDA professional, IMCE, Belgium).

2.3. Evaluation of the uniformity of the filler distribution

The evaluation of the uniformity of the filler distribution was accomplished by a novel image analysis routine using polished cross-sections of sintered specimens. Micrographs (area of 100 x 92 µm², n = 5 to 7 per sample) were recorded by SEM (FEI Quanta 200, 10 kV acceleration voltage) employing a back-scatter electron (BSE) detector. Image analysis was carried out using the freely accessible *ImageJ* software package [8]. Images were binarized using an automated thresholding routine, thus distinguishing between ZrO_2 grains and the mullite matrix. In order to avoid potential bias by binarization artifacts, only ZrO_2 grains with equivalent radii greater than 0.5 µm were used for further processing. The distribution of ZrO_2 grains was evaluated by Voronoi tessellation [9], yielding Voronoi cells around individual grains containing the region of space closer to that grain than to any other grain in the sample. The filler distribution uniformity was assessed using the relative standard deviation of the average Voronoi areas of the distinct micrographs for each specimen. In addition to the calculation of the Voronoi cell size distribution, "heat-maps" were created visualizing the size distribution of Voronoi cells, thus yielding information about the spatial distance between individual ZrO_2 grains. Furthermore, the experimentally determined distribution of Voronoi cell areas was compared to the size distribution of Voronoi cells assuming a random distribution of center points (*i.e.* grains) obtained from the normalized distribution function of Poisson Voronoi cell areas in the two-dimensional case as proposed by Járai-Szabó and Néda [10].

3. Results and discussion

3.1. Green properties

Independent of the mixing procedure, relative green densities between 92 % and 93 % of the theoretical value were observed. However, the resulting green strength values varied considerably. Materials obtained through solvent-free mixing techniques (*DrM* and *MeM*) exhibited lower average strength values with higher variation between individual samples (38 ± 14 MPa and 49 ± 12 MPa, respectively), whereas the solvent-based techniques (*SoC*, *SpC*) resulted in green strengths of 57 ± 4 MPa and 64 ± 4 MPa. SEM investigations showed a rough fracture surface for samples with lower strength, while samples obtained from solvent-based process exhibited a smooth fracture pattern (figure 1).

3.2. Microstructure and evaluation of filler distribution

The microstructure of sintered samples was evaluated by SEM investigations of polished cross-sections (figure 2). In all samples, a continuous mullite matrix with dispersed ZrO_2 grains was present. In comparison to *SoC* and *SpC* samples, *DrM* and *MeM* samples exhibited a more heterogeneous distribution of ZrO_2 grains as well as an increased tendency for cavity formation during polishing, indicating decreased bonding between constituents.

In order to quantitatively and objectively evaluate the uniformity of ZrO_2 grain distribution within the samples, a novel approach was developed using an image analysis routine yielding Voronoi diagrams derived from SEM micrographs (figure 3). By using a Voronoi tessellation operation on binarized images, information about the "sphere of influence" of the corresponding ZrO_2 grains was

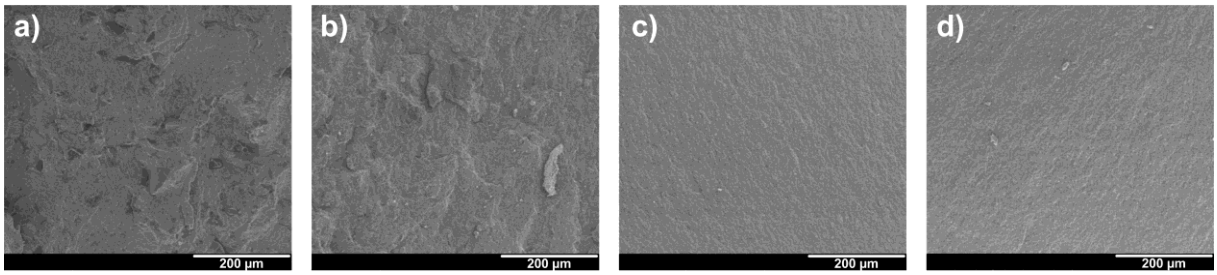

Figure 1. SEM micrographs of fracture surfaces of materials in green state (specimens used for determination of green strength); (a) *DrM*, (b) *MeM*, (c) *SoC*, (d) *SpC*.

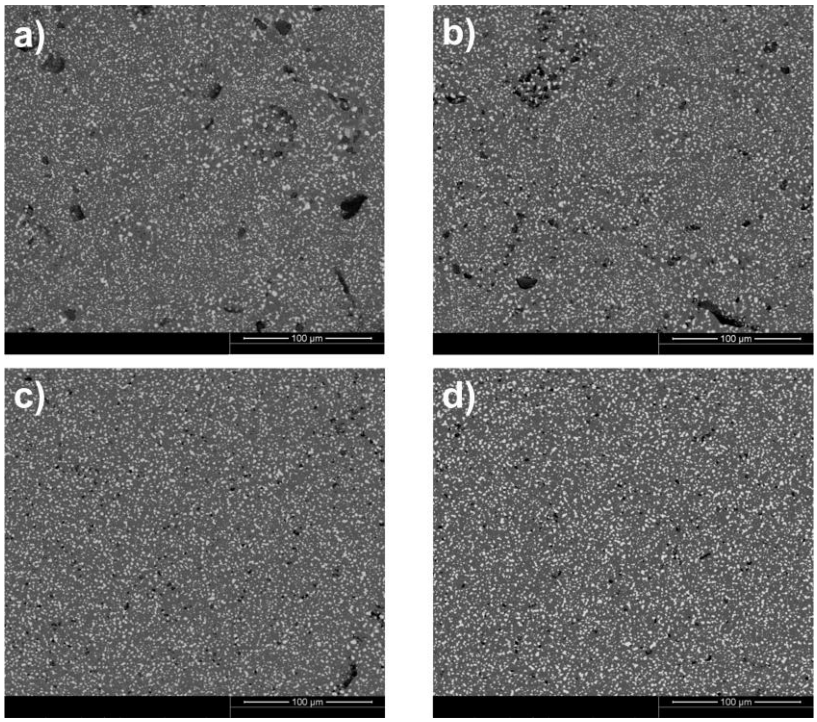

Figure 2. SEM micrographs (BSE detector) of polished cross-sections of sintered materials, with ZrO_2 grains (white) embedded in a mullite matrix (grey); (a) *DrM*, (b) *MeM*, (c) *SoC*, (d) *SpC*.

obtained. By calculation of the relative deviation of the mean Voronoi polygon area obtained for a minimum of five micrographs of the same sample, a direct comparison of the homogeneity of filler distribution within a single sample was obtained (*DrM*: average Voronoi area 10.8 ± 1.7 µm², relative deviation 15 %; *MeM*: 10.1 ± 0.6 µm², 6 %; *SoC*: 12.2 ± 0.9 µm², 7 %; *SpC*: 12.7 ± 0.4 µm², 4 %). Owing to the significantly higher relative deviation of average Voronoi cell areas, the *DrM* sample`s heterogeneity can be considered to be higher than comparable samples obtained through the other mixing methods. The low deviation of the *MeM* sample, comparable to that of *SoC* and *SpC* samples, can be explained by the milling process necessary for breaking up the solid mixture after the mixing step. This leads to a high homogeneity of the filler distribution within the specimen, despite possible local heterogeneities as shown in figure 3b.

By comparison of the experimentally determined normalized size distribution of Voronoi cells with a predicted normalized size distribution obtained from the Poisson Voronoi model [10], a distinction can be made between a quasi-random filler distribution (figure 4a) as opposed to a heterogeneous distribution involving pores and particle clustering. Variations from the random distribution lead to a shift in the distribution function towards higher normalized cell areas (figure 4b).

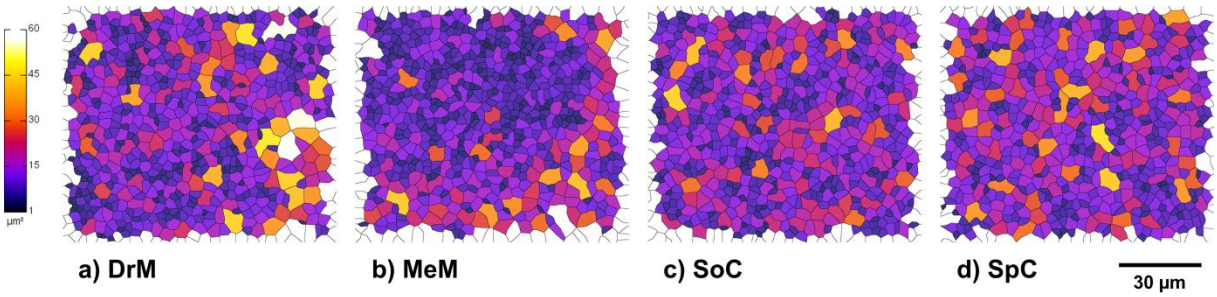

Figure 3. Voronoi diagrams obtained by image analysis of micrographs, the Voronoi cells being color-coded according to the respective cell areas; (a) *DrM*, (b) *MeM*, (c) *SoC*, (d) *SpC*.

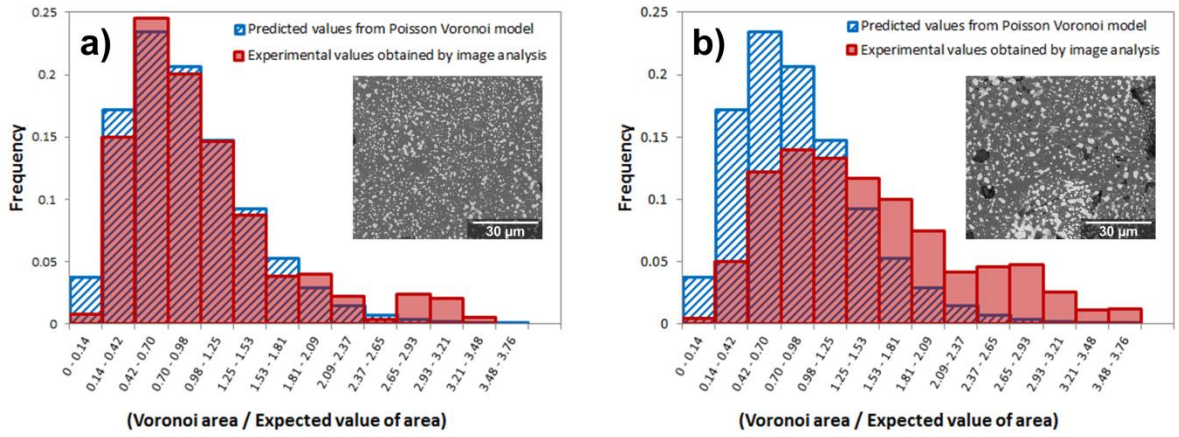

Figure 4. Comparison of the normalized size distribution of Voronoi areas determined by image analysis with predicted values from the Poisson Voronoi model for two distinct micrographs from different regions of the same *DrM* sample, showing a quasi-random filler distribution (a) as opposed to clustering (b); micrographs used for the image analysis routine are shown next to the respective figures.

3.3. Crystalline phase composition, structural and mechanical properties

The more heterogeneous distribution of filler particles in *DrM* samples led to differences in the crystalline phase composition when compared to the rest of the samples (table 1). Significantly higher amounts of unreacted Al_2O_3 and undissociated $ZrSiO_4$ can be observed, indicating spatial separation of reaction partners. In all other samples, the major portion of $ZrSiO_4$ temporarily formed during the heating of the materials is dissociated, thus leading to the formation of mullite in presence of Al_2O_3.

All samples exhibited closed porosities between 7 % and 10 % (table 2). In addition, significant amounts of open porosity were found in *DrM* samples only. In correlation with increased densification

Table 1. Crystalline phase composition of sintered samples calculated from XRD data (estimated absolute error of ± 1 %).

	$3Al_2O_3 \cdot 2SiO_2$ (m.%)	ZrO_2 mon. (m.%)	ZrO_2 tetr. (m.%)	Al_2O_3 (m.%)	$ZrSiO_4$ (m.%)
DrM	65	17	10	4	5
MeM	66	20	9	3	2
SoC	66	21	9	3	1
SpC	66	21	10	2	1

Table 2. Density, porosity, and mechanical properties of sintered samples.

	Bulk density (g cm^{-3})	Porosity[a] (%)	Open porosity (%)	Hardness HV_{10} (GPa)	Fracture toughness (MPa $m^{0.5}$)	Young's Modulus (GPa)
DrM	3.07	17	9	6.4 ± 2.1	-	174 ± 26
MeM	3.43	8	-	8.5 ± 1.5	2.3 ± 0.3	175 ± 11
SoC	3.34	10	-	8.5 ± 0.7	3.7 ± 0.1	157 ± 20
SpC	3.48	7	-	9.0 ± 0.7	3.5 ± 0.2	173 ± 18

[a] calculcated with respect to crystalline phase composition obtained from XRD data

and a higher uniformity of distribution of constituents, an increase in hardness and fracture toughness was observed. Higher scattering of hardness values for *DrM* and *MeM* samples can be related to local microstructural heterogeneities, while more uniform values were found for *SoC* and *SpC* samples. Independent of the chosen mixing technique, Young's moduli between 160 GPa and 180 GPa were found. Mechanical property values determined for samples obtained from solvent-assisted mixing methods are in good accordance with literature data reported for mullite/ZrO_2 composites [4].

4. Conclusions

Polysiloxane/Al_2O_3/ZrO_2 mixtures were successfully transformed into mullite/ZrO_2 composites using a polymer-derived ceramic approach. Solvent-assisted techniques were found to be the method of choice for the introduction of the particulate fillers into the preceramic polymer. While dry mixing of the constituents led to clustering of constituents in the microstructure of the final material, solvent-assisted coating techniques provided for a homogeneous, quasi-random distribution of the particulates within the preceramic polymer matrix, leading to improved mechanical properties in green as well as in sintered state. Spray-coating was shown to be a promising alternative to conventional solvent evaporation from polymer/filler slurries, yielding a ready-to-press composite powder.

A new image analysis approach employing Voronoi tessellation was shown to be a useful tool to quantitatively evaluate the distribution quality of particulates in a PDC matrix. Its applicability was successfully validated by comparison of experimental data with a simulated random distribution following a Poisson process. This technique appears promising not only for the evaluation of filler distributions in PDCs but also for numerous other applications in the field of composite materials.

Acknowledgments

The authors gratefully acknowledge E. Halwax for assistance with XRD investigations.

References

[1] Colombo P, Mera G, Riedel R and Sorarù G D 2010 *J. Am. Ceram. Soc.* **93** 1805–37
[2] Greil P 2000 *Adv. Eng. Mater.* **2** 339–48
[3] Suttor D, Kleebe H J and Ziegler G 1997 *J. Am. Ceram. Soc.* **80** 2541–8
[4] Schneider H and Okada K 2005 Zirconia particle-reinforced composites *Mullite* ed H Schneider and S Komarneni (Weinheim: Wiley-VCH) pp 445–55
[5] Parcianello G, Bernardo E and Colombo P 2011 *J. Am. Ceram. Soc.* **94** 1357–62
[6] Technical data sheet for Silres MK version 1.3, Wacker Chemie AG
[7] Munz D and Fett T 1999 *Ceramics: Mechanical Properties, Failure Behaviour, Materials Selection* (Berlin: Springer) p 36
[8] Schneider C A, Rasband W S, Eliceiri K W 2012 *Nature Methods* **9** 671–5
[9] Okabe A, Boots B, Sugihara K and Chiu S N 2000 *Spatial Tesselations: Concepts and Applications of Voronoi Diagrams* (Chichester: Wiley)
[10] Járai-Szabó F and Néda Z 2007 *Phys.* A **385** 518–26